

Temperature dependence of magnetocrystalline anisotropy constants in the single variant state of L10-type FePt bulk single crystal

著者	及川 勝成
journal or publication title	Applied Physics Letters
volume	88
number	10
page range	102503-1-102503-3
year	2006
URL	http://hdl.handle.net/10097/34935

Temperature dependence of magnetocrystalline anisotropy constants in the single variant state of $L1_0$ -type FePt bulk single crystal

K. Inoue, H. Shima,^{a)} A. Fujita, and K. Ishida

Department of Materials Science, Graduate School of Engineering, Tohoku University, Aoba-yama 02, Sendai 980-8579, Japan

K. Oikawa

Department of Materials Science, Graduate School of Engineering, Tohoku University, Aoba-yama 06, Sendai 980-8579, Japan

K. Fukamichi

Institute of Multidisciplinary Research for Advanced Materials, Tohoku University, Katahira, Sendai 980-8577, Japan

(Received 1 June 2005; accepted 5 January 2006; published online 7 March 2006)

The temperature dependence of magnetocrystalline anisotropy constants and the saturation magnetization in a single variant state have been investigated for $L1_0$ -type $\text{Fe}_{60}\text{Pt}_{40}$ bulk single crystal prepared under compressive stress. The uniaxial magnetocrystalline anisotropy constant K_u evaluated from the magnetization curve is 6.9×10^7 erg cm^{-3} at 5 K. The values of the second- and fourth-order magnetocrystalline anisotropy constants K_1 and K_2 at 5 K determined by the Sucksmith–Thompson method are 7.4 and 0.13×10^7 erg cm^{-3} , respectively. Both the values of K_u and K_1 decrease with increasing temperature T , while K_2 is almost independent of T . The difference between the power law of the Callen and Callen model is described by the dimensionality and the thermal variation of the axial ratio c/a due to the thermal expansion. © 2006 American Institute of Physics. [DOI: 10.1063/1.2177355]

$L1_0$ -type Fe–Pt alloys have attracted much attention because of their large uniaxial magnetocrystalline anisotropy energy (MAE) associated with the long-range ordering of Fe and Pt layers along the c axis.¹ $L1_0$ -type $\text{Fe}_{50}\text{Pt}_{50}$ alloy in a multivariant state exhibits uniaxial magnetocrystalline anisotropy energy of 7.0×10^7 erg cm^{-3} at room temperature.² The large uniaxial magnetocrystalline anisotropy brings about a high thermal stability in magnetic recordings.^{3,4} Since the magnetocrystalline anisotropy constant K_u is a measure for the achievable recording data density, the precise determination of K_u is practically important. Multivariants, twin boundaries and residual stress, and surface and interface anisotropies cause barriers to evaluate the precise K_u for $L1_0$ -type Fe–Pt thin films and nanoparticles. Therefore, $L1_0$ -type Fe–Pt bulk single crystal in a single variant state is necessary for the accurate evaluation of K_u . Furthermore, the investigation on the temperature dependence of the magnetocrystalline anisotropy is meaningful for heat-assisted magnetic recording techniques, because the switching field governed by K_u can be reduced by heating in writing processes.⁵

Face-centered-cubic (fcc)-type Fe–Pt single crystal transforms into an $L1_0$ -type phase, accompanied by multivariant structures because of the reduction of the lattice strain energy. The $L1_0$ -type Fe–Pt single crystal in a multivariant state is insufficient for evaluating accurate K_u because the c axis has three equivalent $\langle 100 \rangle$ directions in the fcc-phase matrix. We have succeeded in preparing $L1_0$ -type Co–Pt (Ref. 6) and Fe–Pd (Refs. 7 and 8) alloys in a single variant state in a wide range of composition by the heat treatment under compressive stress. Fe–Pt alloy is also ex-

pected to transform into an $L1_0$ -type phase in a single variant state by the heat treatment under compressive stress. In the present letter, $L1_0$ -type $\text{Fe}_{60}\text{Pt}_{40}$ single crystal in the single variant state has been prepared in a similar way. It should be noted that $\text{Fe}_{50}\text{Pt}_{50}$ bulk single crystal in a single variant state is difficult to obtain. That is, $\text{Fe}_{50}\text{Pt}_{50}$ has a high-ordering temperature, and hence the preparation at high temperature is necessary, but it induces recovery and recrystallization behaviors.

Magnetizations up to 140 kOe were measured with a vibrating sample magnetometer (VSM) in the temperature range from 5 to 298 K. The value of magnetization was calibrated by the data obtained with a superconducting quantum interference device magnetometer. The Curie temperature was determined from the thermomagnetization curve obtained with the VSM up to 973 K.

Figures 1(a) and 1(b) show the x-ray diffraction patterns with the scattering vector parallel to the a and c axes of the $L1_0$ -type $\text{Fe}_{60}\text{Pt}_{40}$ single crystal, respectively. The reflections are characteristic to $L1_0$ -type single crystals. The fundamental peaks of 200 and 400 are observed in Fig. 1(a). On the other hand, 001 and 003 superlattice peaks, together with the 002 and 004 fundamental peaks, are observed in Fig. 1(b). Since the integrated intensity ratio I_{111}/I_{002} decreased by polishing, a weak 111 peak around $2\theta=43^\circ$ is due to the surface grains with misorientation, which may result from the shear stress distribution at the surface due to the holder contact. The amount of such roughness at the surface is less than 0.1% of the volume of bulk crystal. Accordingly, the present $L1_0$ -type $\text{Fe}_{60}\text{Pt}_{40}$ alloy is in the single-crystal state and the preciseness of magnetocrystalline anisotropy constants is ensured. Since the relative-intensity ratio $I(200)/I(002) \approx 0$ in Fig. 1(b), it is confirmed that the c axis in the $L1_0$ -type $\text{Fe}_{60}\text{Pt}_{40}$ bulk single crystal is uniaxially oriented by the heat-

^{a)}Electronic mail: hisashi@maglab.material.tohoku.ac.jp

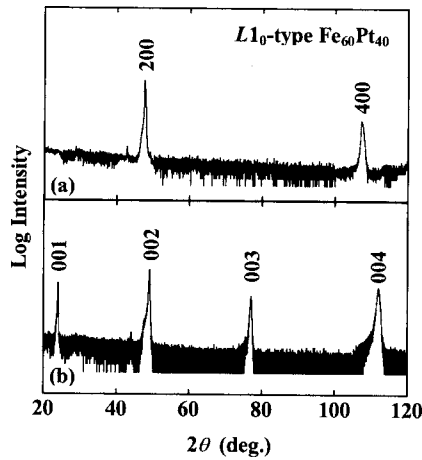


FIG. 1. X-ray diffraction patterns of $L1_0$ -type $\text{Fe}_{60}\text{Pt}_{40}$ bulk single crystal with the scattering vector parallel to (a) the a axis and (b) the c axis.

treatment under compressive stress. Using the single crystal, the MAE of $L1_0$ -type $\text{Fe}_{60}\text{Pt}_{40}$ can be evaluated. The value of the long-range atomic order S was evaluated to be 0.8 by the x-ray diffraction measurement.

Figure 2 shows the magnetization curves at 298 K for the $L1_0$ -type $\text{Fe}_{60}\text{Pt}_{40}$ bulk single crystal in the single variant state. A large magnetocrystalline anisotropy between the magnetization curves along the c and a axes is observed. The magnetization curve along the c axis is easily saturated below 5 kOe, while the saturation along the a axis is achieved above the high magnetic field of about 110 kOe. The values of coercivity H_c along the c and a axes are about 450 and 350 Oe, respectively. The value of H_c along the c axis is much smaller than that of $L1_0$ -type Fe–Pt bulk alloy in the multi-variant state, and also thin films and nanoparticles.^{9–11}

The magnetocrystalline anisotropy constant K_u is directly obtained from the following difference between the magnetization curves along the easy and hard axes:

$$K_u = \int_0^{M_s} (H_{\text{eff}}^{a\text{-axis}} - H_{\text{eff}}^{c\text{-axis}}) dM, \quad (1)$$

where H_{eff} is the effective magnetic field defined as $H_{\text{ex}} - NM$. Here, H_{ex} is the external magnetic field and N and M are the demagnetization factor and magnetization, respectively. High magnetic field measurements are important to achieve the saturation of magnetization along the hard axis for the determination of K_u by using Eq. (1). On the other hand, in a

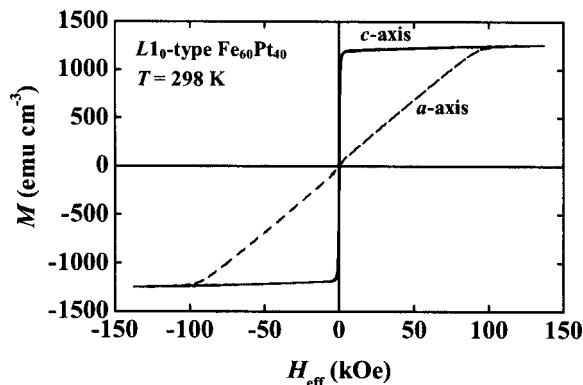


FIG. 2. Magnetization curves at 298 K for $L1_0$ -type $\text{Fe}_{60}\text{Pt}_{40}$ bulk single crystal in the single-variant state. The solid and dashed curves represent the values measured along the c and a axes, respectively.

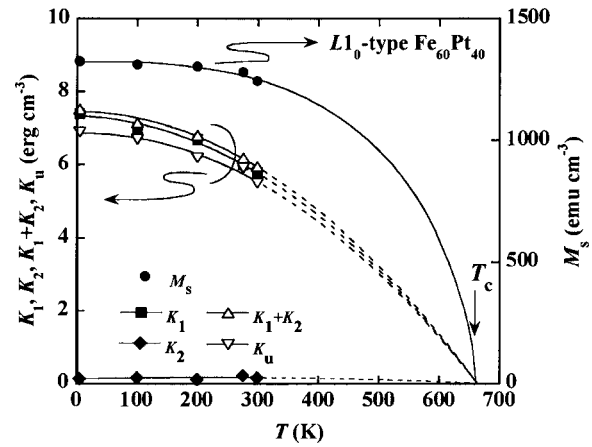


FIG. 3. Temperature dependence of the second- and fourth-order magneto-crystalline anisotropy constants K_1 and K_2 , K_1+K_2 together with K_u , and the saturation magnetizations M_s for $L1_0$ -type $\text{Fe}_{60}\text{Pt}_{40}$ bulk single crystal in the single-variant state. The solid line denotes the extrapolation by the Brillouin function within the molecular field approximation for the momentum quantum number $J=1$, and the Curie temperature $T_c=663$ K.

coherent rotation process independent of the magnetic domain-wall motion, the MAE in tetragonal crystal systems with the uniaxial symmetry depends on the polar angle θ between the magnetization and the c axis: $E_{\text{MAE}}(\theta) = K_1 \sin^2 \theta + K_2 \sin^4 \theta + \dots$. The values of K_1 and K_2 can be evaluated by applying the Sucksmith–Thompson (ST) method¹² given by Eq. (2) to the high-field magnetization data along the a axis:

$$\frac{H_{\text{eff}}}{M} = 2K_1 \frac{1}{M_s^2} + 4K_2 \frac{M^2}{M_s^4}. \quad (2)$$

In the present letter, K_u , K_1 , and K_2 have been determined by using Eqs. (1) and (2).

Shown in Fig. 3 is the temperature dependence of K_1 , K_2 , K_1+K_2 , and K_u , together with M_s evaluated by the law of approach to saturation. Compared with K_1+K_2 , the value of K_u obtained from the data in Fig. 2 is reduced due to the contribution from magnetic domain walls under low magnetic fields. Magnetic domain-wall displacements generally dominate the magnetization process under low magnetic fields. The values of K_1 , K_2 , and K_u at 5 K are evaluated to be 7.4×10^7 erg cm^{-3} , 0.13×10^7 erg cm^{-3} , and 6.9×10^7 erg cm^{-3} , respectively. The present values of K_1+K_2 and K_u are larger than those of $L1_0$ -type CoPt (Ref. 6) and FePd (Ref. 7) single crystals in the single-variant state. $L1_0$ -type $\text{Fe}_{60}\text{Pt}_{40}$ alloy has large magnetocrystalline anisotropy constants despite the deviation from the equiatomic composition. The second-order magnetocrystalline anisotropy constant K_1 and the uniaxial magnetocrystalline anisotropy constant K_u monotonically decreases with increasing temperature. However, both K_1 and K_u keep a large value up to 298 K, being 6.0×10^7 erg cm^{-3} and 5.5×10^7 erg cm^{-3} , respectively. The fourth-order magnetocrystalline anisotropy constant K_2 is much smaller than K_1 , almost independent of temperature. The saturation magnetization $M_s(T)$ decreases with increasing temperature, being 1245 emu cm^{-3} at 298 K.

According to the single-ion model by Callen and Callen,¹³ the temperature dependence of K_1 is related to that of M_s as follows:

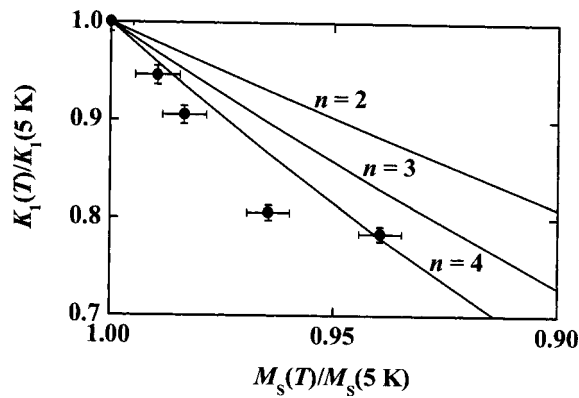


FIG. 4. The relation between the magnetocrystalline anisotropy constant K_1 and the saturation magnetization M_s normalized to the values at 5 K. The solid circles represent the observed values of $\text{Fe}_{60}\text{Pt}_{40}$ single crystal in the single-variant state, and three solid lines correspond to $n=2, 3$, and 4 [in Eq. (3)].

$$K_1(T)/K_1(0) = [M_s(T)/M_s(0)]^n. \quad (3)$$

In Fig. 4, the relation between the magnetocrystalline anisotropy constant K_1 and the saturation magnetization M_s normalized to the values at 5 K is given for the $\text{Fe}_{60}\text{Pt}_{40}$ single crystal in the single-variant state. The solid circles stand for the experimental results. The lines designate $n=2, 3$, and 4 in Eq. (3). It is noted that $n=3$ for the uniaxial symmetry, such as $L1_0$ -type crystal structure. However, the present result obtained from Fig. 4 is close to the behavior with $n=4$. In addition, available values of n for $L1_0$ -type Fe-Pt thin films are smaller than 3; close to 2.^{14,15} The $L1_0$ -type Fe-Pt bulk single-crystal, nanoparticle¹⁶ and epitaxial thin films^{14,15} exhibit the different value of n , although they have the same $L1_0$ -type crystal structure with $c/a < 1$. The temperature dependence of $M_s(T)/M_s(0)$ in Eq. (3) depends on the dimensionality, because the wave number of the thermally excited spin wave depends on the dimensionality.^{17–19} The temperature dependence of $M_s(T)$ in the single-variant state for $L1_0$ -type $\text{Fe}_{60}\text{Pt}_{40}$ bulk single crystal is comparable with the Brillouin function for the momentum quantum number $J=1$ as shown by the solid line in Fig. 3. In contrast, Okamoto *et al.*¹⁴ have reported that the value of J becomes 6–10 for $\text{FePt}(001)$ epitaxial film. The temperature dependence of $M_s(T)/M_s(0)$ in Eq. (3) for bulk ferromagnetic alloys decreases slower than that for ferromagnetic alloy in thin films with increasing temperature in contrast to the similar temperature dependence of $K_1(T)/K_1(0)$. Especially in the present system, the spin wave excitation is influenced by the twin boundary in multivariant state. As a result, the values of n of nanoparticles and epitaxial films are deviated from the Callen and Callen model¹³ due to various extrinsic influences. On the other hand, the large value of n compared with the ideal model for the bulk single crystal in the single-variant state would be attributed to the contribution from the characteristics in the thermal expansion of the a and c axes. Namely, the axial ratio of c/a decreases with increasing temperature.²⁰ According to the first-principles calculation, K_u decreases,¹ whereas M_s increases with decreasing c/a .²¹ As a result, the larger value of n compared with the value

obtained from the single-ion model is expected from Eq. (3). Such a difference between the power law of the Callen and Callen model¹³ for the $L1_0$ -type Fe-Pt alloy is figured out only when the bulk single crystal in the single-variant state is used.

In conclusion, $L1_0$ -type $\text{Fe}_{60}\text{Pt}_{40}$ bulk single crystal in the single-variant state has been prepared by heat treatment under compressive stress, and the temperature dependences of the magnetocrystalline anisotropy constant K_u and the saturation magnetization M_s are discussed. The magnetization along the a axis is completely saturated under the magnetic field of about 110 kOe at 298 K. The value of K_u at 5 K directly evaluated from magnetization curves is of $6.9 \times 10^7 \text{ erg cm}^{-3}$. The values of the second- and fourth-order magnetocrystalline anisotropy constants K_1 and K_2 at 5 K determined by the ST method are $7.4 \times 10^7 \text{ erg cm}^{-3}$ and $0.13 \times 10^7 \text{ erg cm}^{-3}$, respectively. Both the values of K_u and K_1 decrease with increasing temperature T , while K_2 is almost independent of T . The difference between the power law of the Callen and Callen model¹³ for $L1_0$ -type Fe-Pt alloys is explained by the dimensionality and the thermal variation of the axial ratio c/a due to the thermal expansion.

The authors acknowledge Professor T. Nojima and Dr. S. Nakamura of the Center for Low Temperature Science, Tohoku University for their support with the high magnetic field measurements.

- ¹A. Sakuma, J. Phys. Soc. Jpn. **63**, 3053 (1994).
- ²O. A. Ivanov, L. V. Solina, V. A. Demshina, and L. M. Magat, Phys. Met. Metallogr. **35**, 81 (1973).
- ³A. Moser, K. Takano, D. T. Margulies, M. Albrecht, Y. Sonobe, Y. Ikeda, S. Sun, and E. E. Fullerton, J. Phys. D **35**, R157 (2002).
- ⁴D. Weller and A. Moser IEEE Trans. Magn. **35**, 4423 (1999).
- ⁵J. J. M. Ruigrok, R. Coehoorn, S. R. Cumpson, and H. W. Kesteren, J. Appl. Phys. **87**, 5398 (2000).
- ⁶H. Shima, K. Oikawa, A. Fujita, K. Fukamichi, and K. Ishida, Appl. Phys. Lett. **86**, 112515 (2005).
- ⁷H. Shima, K. Oikawa, A. Fujita, K. Fukamichi, and K. Ishida, J. Magn. Magn. Mater. **272**, 2173 (2004).
- ⁸H. Shima, K. Oikawa, A. Fujita, K. Fukamichi, K. Ishida, and A. Sakuma, Phys. Rev. B **70**, 224408 (2004).
- ⁹Y. Ding, S. Yamamuro, D. Farrell, and S. A. Majetich, J. Appl. Phys. **93**, 7411 (2003).
- ¹⁰B. C. Lim, J. S. Chen, and J. P. Wang, J. Magn. Magn. Mater. **271**, 159 (2004).
- ¹¹K. Na, J. G. Na, H. J. Kim, P. W. Jang, and S. R. Lee, IEEE Trans. Magn. **37**, 1302 (2000).
- ¹²W. Sucksmith and J. E. Thompson, Proc. R. Soc. London, Ser. A **225**, 362 (1954).
- ¹³E. R. Callen and H. B. Callen, J. Phys. Chem. Solids **16**, 310 (1960).
- ¹⁴S. Okamoto, N. Kikuchi, O. Kitakami, T. Miyazaki, Y. Shimada, and K. Fukamichi, Phys. Rev. B **66**, 024413 (2002).
- ¹⁵J.-U. Thiele, K. R. Coffey, M. F. Toney, J. A. Hedstrom, and A. J. Kellock, J. Appl. Phys. **91**, 6595 (2002).
- ¹⁶X. W. Wu, K. Y. Guslienko, R. W. Chantrell, and D. Weller, Appl. Phys. Lett. **82**, 3475 (2003).
- ¹⁷J. A. Davis and F. Keffer, J. Appl. Phys. **34**, 1135 (1963).
- ¹⁸P. Crespo, J. M. González, A. Hernando, and F. J. Yndurain, Phys. Rev. B **69**, 012403 (2004).
- ¹⁹E. Della Torre, L. H. Bennett, and R. E. Watson, Phys. Rev. Lett. **94**, 147210 (2005).
- ²⁰Y. Tsunoda and H. Kobayashi, J. Magn. Magn. Mater. **272**, 776 (2004).
- ²¹J. B. Staunton, S. Ostanin, S. S. A. Razee, B. Gyroffly, L. Szunyogh, B. Ginatempo, and E. Bruno, J. Phys.: Condens. Matter **16**, S5623 (2004).